Langmuir

Article

pubs.acs.org/Langmuir

Nematic Ordering of SWNT in Meso-Structured Thin Liquid Films of Polystyrenesulfonate

Racheli Itzhak-Cohen,[†] Einat Nativ-Roth,[‡] Yael Levi-Kalisman,[‡] Elinor Josef,[§] Igal Szleifer,[∥] and Rachel Yerushalmi-Rozen*[,†,‡]

[†]Department of Chemical Engineering, [‡]The Ilse Katz Institute for Nanoscale Science and Technology, Ben-Gurion University of the Negev, Beer Sheva 84105, Israel

[§]Department of Chemical Engineering, Technion, Haifa 32000, Israel

[∥]Department of Biomedical Engineering, Northwestern University, 2145 Sheridan Road, Evanston, Illinois 60208, United States

Supporting Information

ABSTRACT: The formation of nematic-like islands of single-walled carbon nanotubes (SWNT) in polystyrenesulfonate (PSS) dispersions confined into nanometrically thin films is reported. The SWNT are observed to assemble into orientationally ordered phases, where the intertube distance, as measured via transmission electron microscopy at cryogenic temperatures, matches the polyelectrolyte's bulk correlation length deduced from X-ray scattering. The micrometers-long islands of orientationally ordered carbon nanotubes are observed in both SWNT and double-walled carbon nanotubes (DWNT) but not in specimens prepared from similar dispersions of multiwalled carbon nanotubes (MWNT). These observations, together with relaxation and rheological experiments, suggest that the orientational ordering may result from coupling between confinement of the polymer-wrapped SWNT and DWNT and the microstructure of the solvated polyelectrolyte.

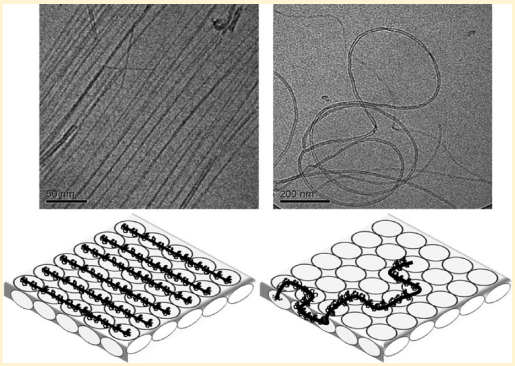

INTRODUCTION

Self-assembly of carbon nanotubes (CNT) into orientationally ordered phases in thin films is a compelling topic with technological applications that rely on the nonisotropic response of the resulting materials to electromagnetic radiation, heat conductance, and mechanical properties.[1]

Single-walled carbon nanotubes (SWNT) are characterized by a unique combination of electrical and mechanical properties.[2−4] Individual SWNT are elongated cylinders with diameters of 1−2 nm and lengths that may reach tens to hundreds of micrometers. Theoretical predictions and mechanical measurements of the modulus of defect-free SWNT indicate very large persistence lengths (32−174 μm),[5] suggesting that individual SWNT should behave as rigid rods. Multiwalled carbon nanotubes (MWNT), comprising concentric cylinders of graphene with a diameter in the range of 3 to about 100 nm and grown via chemical vapor deposition (CVD), are characterized by a random distribution of defects along the tube, which significantly reduce the rigidity of the tube as compared to that of an ideal, defect-free CNT.[6]

A dispersion of CNT in aqueous media is a prerequisite for their processing. Yet, due to the high contact energy among the tubes (about 35 k_BT/nm, in vacuum),[7] SWNT tend to assemble into large van der Waals (vdW) crystals, known as bundles. The bundles are insoluble in liquids, posing a hurdle for utilization of CNT in most applications. Several approaches were proposed for dispersing individual CNT in aqueous solutions, among which is the noncovalent adsorption of charged polymers, polyelectrolytes (PE).[8−10] CNT dispersion by a common polyelectrolyte, polystyrenesulfonate (PSSNa), was first described by O'Connell et al.[11] and suggested that the polymers wrap around the CNT.

The solution behavior of PE is complex due to the long-range nature of the electrostatic interactions as well as the presence of counterions in the solution.[12] Scaling theories,[12,13] which outline the phase behavior of PE as a function of their concentration, introduced the terms used to describe the structure and behavior of PE solutions: At very low PE concentrations, interchain interactions may be neglected. As the concentration is increased, it reaches the overlap concentrations, c^*, where interchain interactions become important. Here, the relevant length scale is the correlation length ξ, the mesh size of a net-like structure formed by the solvated chains due to the onset of an excluded volume from which other segments are partly expelled. Scattering experiments, particularly small-angle X-ray scattering (SAXS), of PE solutions show a single broad maximum in the scattering intensity at a

Received: August 22, 2014
Revised: November 22, 2014
Published: November 24, 2014

   dx.doi.org/10.1021/la503287q | *Langmuir* 2014, 30, 14963−14970

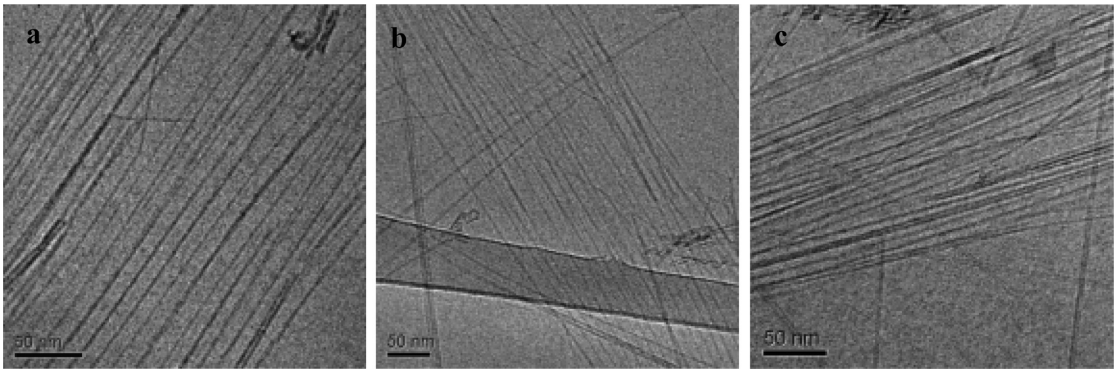

Figure 1. Cryo-TEM images of SWNT (dark lines in the image) dispersed in aqueous solutions of (a) 2 wt % PSSNa 126.7 kg/mol, (b) 3 wt % PSSH 75 kg/mol, and (c) 5 wt % PSSH 75 kg/mol. The scale bars are 50 nm.

wave vector q_{max} that is directly related to the correlation length as $\xi = 2\pi/q_{max}$.[13,14]

Although previous studies focused on the ability of PE to disperse SWNT,[1,11,15] here, we report the behavior of the combined system under strong confinement. We report the formation of nematic-like islands of SWNT in thin films of PSS dispersions where the intertube spacing is determined by the correlation length of the polymer. We suggest that the orientational ordering results from the combination of PSS-wrapped SWNT, which behave as rigid rods, confinement, and the microstructure of the PSS solution.

Theories describing the behavior of rigid rods in bulk solutions have been proposed by Onsager[16] and Flory.[17,18] Onsager described the phase behavior of idealized monodisperse rods interacting via a mean field excluded-volume potential in an athermal solvent. This theory is based on the competition between the orientational entropic contribution to the free energy and the excluded-volume potential. Flory's lattice-based theory[17] also explains the rigid rod phase behavior, which accounts for excluded-volume interactions via packing effects and allows for attractive interparticle interactions governed by the quality of the solvent. Both theories describe the phase transition of rigid rods solutions from an isotropic solution, where rods are randomly oriented, to an orientationally ordered liquid phase (liquid crystal), where both translation and rotation are inhibited as rods crowd beyond a critical concentration. Between these two, a biphasic region exists where a liquid crystal phase is in equilibrium with the isotropic phase. Liquid-crystalline phases of pristine SWNT in superacids,[19−21] sidewall-functionalized CNT, and DNA-stabilized MWNT in water were reported.[22,23] In addition, a nematic phase was reported by Islam et al. when CNT were trapped within temperature-sensitive cross-linked hydrogels.[24]

The micrometers-long islands of orientationally ordered SWNT observed here in nanometric thin films of PSS solutions appear at SWNT concentrations below 0.5 wt %, only in dispersions of SWNT and DWNT, and not in dispersions of MWNT. Moreover, the intertube spacing of the nematic islands is strongly correlated to the microstructure of the polymer solutions and thus may be tuned by the polymer concentration. We discuss the origins of the observed behavior and relate them to the solution behavior of confined rod-like objects embedded in nonconfined PE solutions.

EXPERIMENTAL SECTION

Carbon Nanotubes (CNT). Raw CNT powders were purchased from different sources and used as received. Their characteristics are given in the Supporting Information, Table S1.

Polymers. Sodium polystyrenesulfonate (PSSNa), ammonium polystyrenesulfonate ($PSSNH_3$) (product no. 690405001), and lithium polystyrenesulfonate (PSSLi) (product no. 690422001) were purchased from Scientific Polymer Products, Inc. (http://scientificpolymer.com/). The fraction of sulfonated styrene monomers (f) and the molecular mass (MW), as reported by the manufacturer, are presented in the Supporting Information, Table S2. Polystyrene sulfonic acid (PSSH) (product no. MKBP9562V) was purchased from Sigma (Israel).

Salts. NaCl was purchased from Bio Lab (Israel) (product no. 905921). NaOH was purchased from Bio Lab (product no. 793531).

Preparation of Solutions and Dispersions. Aqueous polyelectrolyte solutions in concentrations of 0.1−10 wt % (polyelectrolyte in water) were prepared by dissolving the polyelectrolyte in deionized water (Millipore water, resistance of 18.2 MΩ cm) and heating (50 °C for 1 h); after incubation for 2 days, the solution was filtered by a 0.22 μm pore size filter (Merck Millipore Inc.). Dispersions of CNT were prepared by sonicating raw CNT powder (typical concentration of 0.1−0.5 wt %) in polyelectrolyte solutions under very mild conditions (50 W, 43 kHz) for 90−120 min. The dispersions were centrifuged (at 4500 rpm for 20 min), and the supernatant was decanted from above the precipitate. As was shown before,[25] the dispersion process is selective toward CNT, and the precipitate contains mainly colloidal moieties. Yet, we estimate that some of the CNT precipitates, so the actual weight percent of the dispersed CNT is lower than the initial concentration designated throughout the text. NaOH or NaCl in the desired concentration was added to the dispersion.

Transmission Electron Microscopy at Cryogenic Temperatures (Cryo-TEM). Dispersions were characterized via direct imaging using cryo-TEM. Samples were prepared by depositing a droplet of 2−4 μL on a TEM grid (300 mesh Cu Lacey grid; Ted Pella Ltd.). Ultrathin films (100−150 nm)[27] were formed as most of the solution was removed by blotting. The specimen was vitrified by rapid plunging into liquid ethane precooled with liquid nitrogen at controlled temperature and relative humidity (Leica EM GP). The vitrified samples were transferred to a cryo-specimen holder (Gatan model 626) and examined at −181 °C in low-dose mode. Imaging was carried out using FEI Tecnai 12 G^2 TEM equipped with Gatan 794 CCD camera and operated at 120 kV.

Small Angle X-ray Scattering (SAXS). The nanoscale organization of the polymer solutions and the CNT dispersions was characterized using SAXS. The sample was placed in a disposable quartz capillary with diameter of about 1.5 mm and sealed with epoxy glue. The SAXS measurements were performed with SAXLAB's GANESHA 300 XL. The scattering vector $q = (4\pi/\lambda_0) \sin \theta/2$ ranged from 0.012 to 0.67A^{-1}. The results were converted from 2D to 1D via SAXSGUI. The intensity is presented in absolute units; the scattering curves were corrected for measuring time, incident intensity, sample

dx.doi.org/10.1021/la503287q | Langmuir 2014, 30, 14963−14970

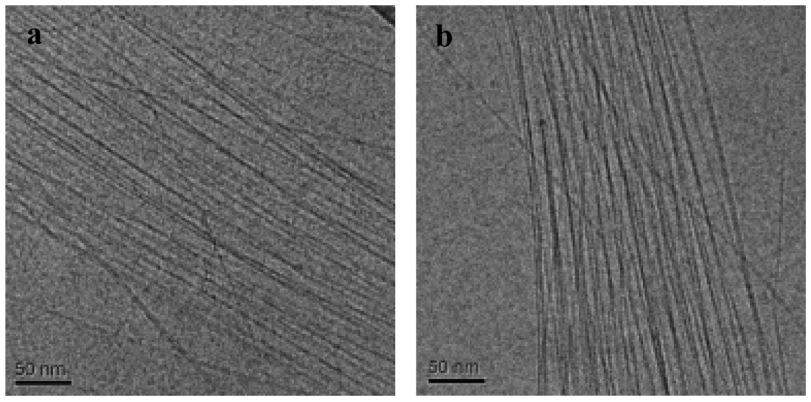

Figure 2. Cryo-TEM images of SWNT dispersed in (a) 2 wt % PSSLi 70 kg/mol and (b) 2 wt % $PSSNH_3$ 120 kg/mol. The scale bars are 50 nm.

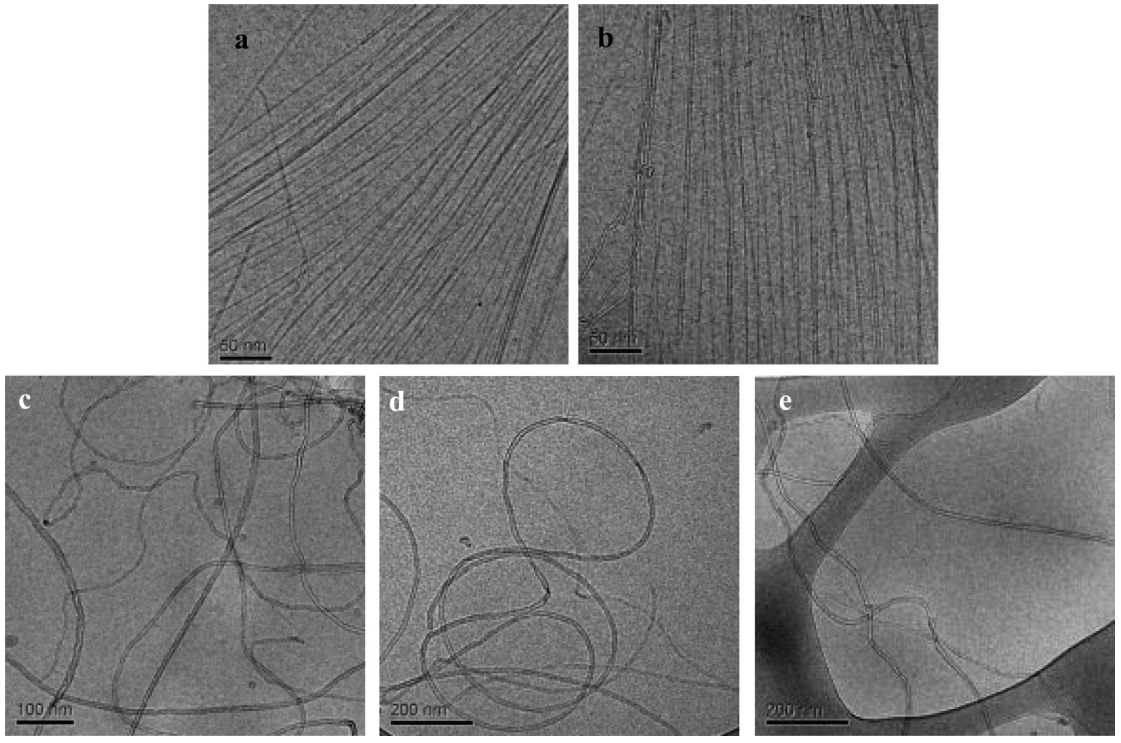

Figure 3. Cryo-TEM images of (a) DWNT dispersed in 2 wt % PSSNa 34.7 kg/mol, (b) DWNT dispersed in 2 wt % PSSNa 126.7 kg/mol, (c) MWNT (Sky Spring) dispersed in 2 wt % PSSNa 126.7 kg/mol, (d) MWNT (Sky Spring) dispersed in 2 wt % PSSH 75 kg/mol, and (e) MWNT (Arkema) dispersed in 2 wt % PSSNa 262.6 kg/mol. Scale bars are (a, b) 50 nm, (c) 100 nm, and (d, e) 200 nm.

transmission, distance from sample to detector, sample thickness, and scattering from the solvent.

Rheological Measurement. Rheological measurements were performed using DHR-2 rotational rheometer (TA Instruments, USA) operated in shear-rate-controlled mode. Steady-state shear measurements in the range of 1−1000 s^{-1} were carried out in parallel-plate geometry (plate diameter 40 mm) at a plate separation gap of 0.5 mm. Each point was measured for 30 s, with 5 s for equilibration.

RESULTS

SWNT (0.5 wt %) were dispersed in PSS solutions at polymer concentrations ranging from 2 to 8 wt %. The dispersions spontaneously demixed into two macroscopic phases: an upper (transparent) minor phase and a lower (black) major phase. The lower phase was enriched with well-dispersed individual SWNT and small bundles (as indicated by cryo-TEM and SAXS), whereas the upper phase was depleted of nanotubes. Similar demixing was observed in dispersions of double-walled carbon nanotubes (DWNT) and multiwalled carbon nanotubes (MWNT) and in polymer dispersions of different counterions (PSSNa, PSSH, PSSLi, and $PSSNH_3$).

Nanometrically thin films, prepared from the lower phase of PSS-SWNT dispersions, were studied using cryo-TEM. In Figure 1a−c, we present images taken from dispersions of SWNT in PSSNa (MW of 126.7 kg/mol) and PSSH (MW of 75 kg/mol) at different concentrations. The images clearly show micrometers-long islands (in the length of the SWNT) of orientationally ordered SWNT. The islands of aligned SWNT coexist with regions of randomly oriented SWNT. Similar images were observed in specimens prepared from dispersions of PSSNa (MW of 16, 57.5, 262.6, 505.1, and 829.1 kg/mol) (Figure S1, Supporting Information), PSSH (MW of 75 kg/mol), and PSSLi (MW of 70 kg/mol), and $PSSNH_3$ (MW of 120 kg/mol) (Figure 2).

dx.doi.org/10.1021/la503287q | *Langmuir* 2014, 30, 14963−14970

Dispersions of DWNT with a typical diameter of 3 nm and MWNT with diameters ranging from 6 to about 20 nm were dispersed in aqueous solutions of PSSNa (126.7 kg/mol, 2 wt %). Cryo-TEM specimens were prepared from the lower phase of the dispersions. We found that although the DWNT formed regimes of coaligned tubes with typical intertube distances similar to those of the SWNT (Figure 3a,b) a similar phenomenon was not observed for MWNT. Rather, cryo-TEM images show random orientation of the dispersed MWNT at PSSNa concentrations ranging from 2 to 5 wt % (Figure 3c–e).

The cryo-TEM images reveal that the SWNT are aligned almost parallel to each other with a typical intertube separation that depends on the bulk concentration of the PSS. SWNT dispersions of PSS at different molecular weights and monovalent counterions show similar behavior. Quantitative analysis of cryo-TEM images indicates that the intertube distance decays from 14 (±3) nm to 6 (±2) nm as the bulk PSS (PSSNa and PSSH, SWNT and DWNT) concentration increases from 2 to 8 wt % (Figure 4).

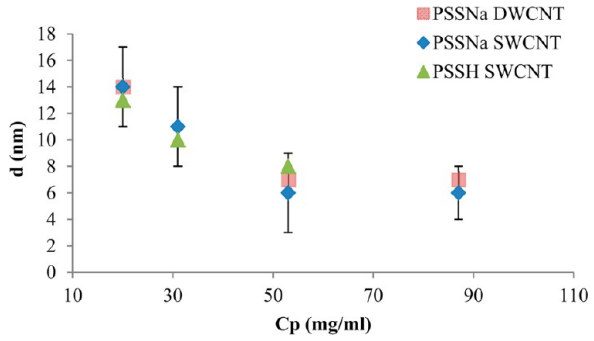

Figure 4. Intertube distance of CNT (derived from cryo-TEM) vs PSSNa 126 kg/mol and PSSH 75 kg/mol. The error bars are derived from an average taken over multiple samples.

The specimens examined by cryo-TEM are obtained by blotting a micrometer-sized droplet of dispersion into an ultrathin liquid film (typical thickness 100–150 nm) via the application of high shear rates (10^3 to 10^6 s^{-1}).[26,27] Hence, one should note that the observed phases have been formed under a combination of high shear rate and strong confinement. As was shown before,[26,28] flow fields that develop during shearing may cause alignment of nanostructures in the liquid specimen prior to vitrification of the sample. In cases of shear-induced structuring, disruption of the structure and randomization are expected when the specimen is allowed to relax to periods of some tens of seconds.[29,30] To test the effect of shear on the formation of aligned SWNT islands, we performed two series of experiments: In the first, the samples were incubated for up to 90 s in a controlled environment after blotting and prior to quench-cooling to allow on-the-grid relaxation. Cryo-TEM images of relaxed specimens of 60 s (Figure 5) and 90 s (Figure S2, Supporting Information) suggest that the alignment of the nematic-like regions is preserved and that randomization of the aligned SWNT does not take place. We note here that during the relaxation process the confinement of the dispersions within a nanometrically thin layer is not relieved.

In a second set of experiments, the steady shear viscosity as a function of the applied shear rate was investigated in bulk solutions at polymer concentrations similar to those investigated via cryo-TEM. In particular, dispersions of SWNT in PSSNa 126.7 kg/mol at a polymer concentration of 5 wt % were prepared as described above, and the rheological properties of the lower phase were examined using a parallel-plate configuration (Figure S3, Supporting Information). The solution showed Newtonian behavior; it is clear that the addition of SWNT to PSS solutions does not modify the rheological characteristics of the PE solution and that both the viscosity and the dependence on the shear rate are almost identical to those of the native solution. Similar results were obtained in previous studies for a 0.1 wt % SWNT dispersion in 10 and 15 wt % pluronic block copolymers.[31] These results are different from the rheological behavior of aqueous dispersions of SWNT (of similar concentration) in solutions of the cationic surfactant cetyltrimethylammonium bromide (CTAB). Cryo-TEM specimens prepared from these dispersions showed shear-induced structuring,[28] and the corresponding bulk rheology[31] showed a dramatic increase in the low shear-rate viscosity of SWNT dispersions and shear thinning behavior at low CTAB concentrations. This behavior was interpreted as resulting from the shear-induced formation of oriented CTAB micelles.[29,31]

The bulk microstructure of the native solutions and dispersions was examined using SAXS. The scattering curves of the native polyelectrolyte solutions are shown in Figure 6a, and the correlation length ξ, as calculated from the maximum peak position $\xi = 2\pi/q_{max}$, in Figure 6b. ξ is expected to scale

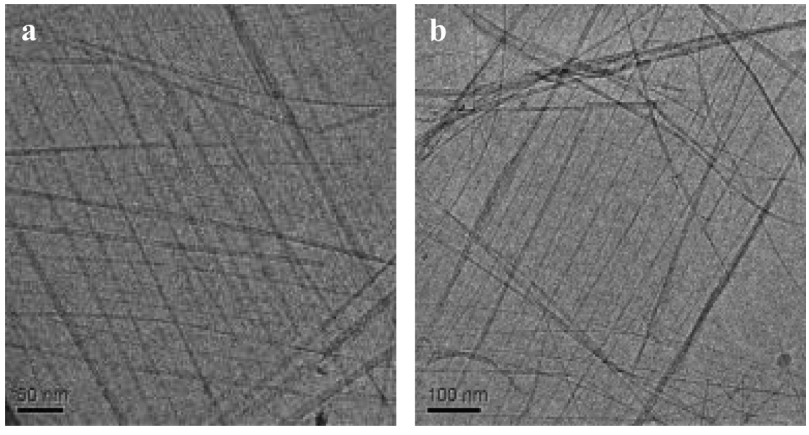

Figure 5. Cryo-TEM images of 0.5 wt % SWNT dispersed in a 0.5 wt % PSSNa 126.7 kg/mol solution following on-the-grid relaxation periods of (a) 0 s and (b) 60 s. Scale bars are (a) 50 nm and (b) 100 nm.

dx.doi.org/10.1021/la503287q | *Langmuir* 2014, 30, 14963–14970

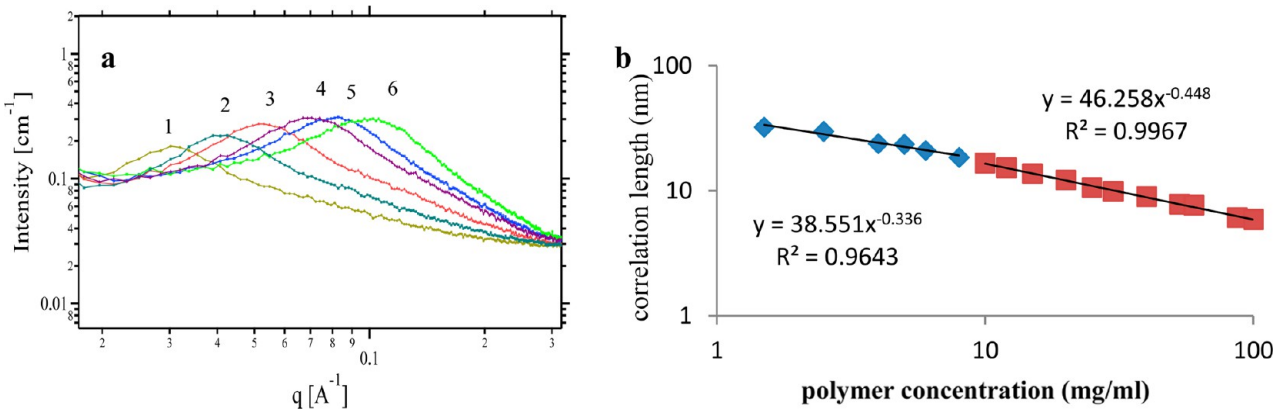

Figure 6. (a) SAXS intensity as a function of the wave vector q of PSSNa 126.7 kg/mol. The different colors represent different concentrations (mg/mL): (1) 6, (2) 12, (3) 20, (4) 40, (5) 53, and (6) 87 (absolute intensity, before background subtraction). (b) Logarithmic plot of the correlation length (ξ) vs PSSNa 126.7 kg/mol.

with polymer concentration as $c^{-1/3}$ in the dilute regime and as $c^{-1/2}$ in the semidilute regime.[12,32] We observe a crossover from $c^{-0.34}$ to $c^{-0.45}$ at a concentration of 8 mg/mL (0.8 wt %) for PSSNa 126.7 kg/mol. A similar transition was observed for PSSH 75 kg/mol and PSSNa 34.7 kg/mol at concentration of 10 mg/mL (1 wt %) (Figures S4 and S5, Supporting Information).

Figure 7 presents scattering curves of SWNT dispersions in PSSNa solutions. Similar results were obtained for DWNT and MWNT, as shown in Figures S6 and S7 in the Supporting Information. The scattering from all CNT dispersions is similar to the scattering from PSSNa solutions at the same polymer concentration. The major difference between the scattering curves is a stronger upturn at low q values of CNT dispersions. This could indicate formation of large clusters or buildup of attractive polymer−CNT/CNT−CNT interactions. The SAXS results do not provide any evidence for the existence of nematic-like islands. Yet, the absence of such evidence cannot exclude the presence of randomly distributed nematic-like islands in the bulk solutions. A more refined analysis of the scattering from SWNT dispersions in PSSNa solutions should be performed in the future using small-angle neutron scattering to obtain further insight into this system.

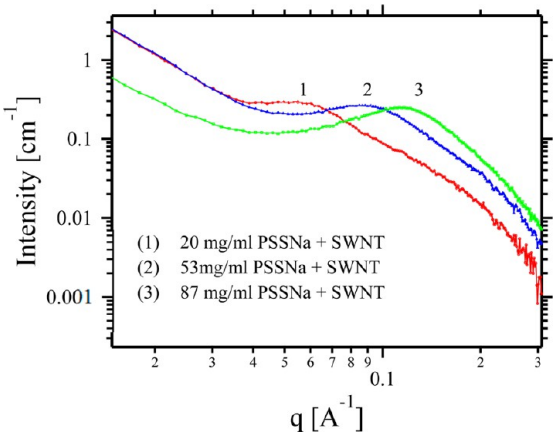

Figure 7. SAXS intensity as a function of the wave vector q obtained from a 0.5 wt % SWNT dispersion in 20 mg/mL (2 wt %), 53 mg/mL (5 wt %), and 87 mg/mL(8 wt %) PSSNa 126.7 kg/mol solutions (absolute intensity, after background subtraction).

In Figure 8, we plot the intertube distance of SWNT islands, as measured in cryo-TEM images, together with the correlation length derived from SAXS experiments as a function of the concentration of PSSNa. At these concentrations, the bulk polymer solutions are in the semidilute regime. We observe that the intertube distance between the SWNT measured in the vitrified thin films is similar to the correlation length of the PSS derived from SAXS measurements of the bulk solution of the polyelectrolyte. This result is consistent in different types of SWNT and DWNT (not shown). Moreover, the correlation length and the intertube distance are similar in semidilute solutions of PE with different molecular masses and counterions (H^+, Na^+)

The apparent correlation between the microstructure of the PE solutions and the intertube distance of coaligned SWNT in confined thin films is the key observation of this study. Its

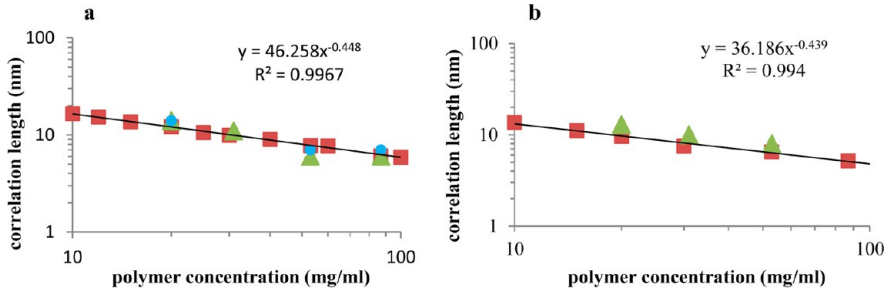

Figure 8. Logarithmic plot of the correlation length (derived from SAXS results) (red squares) and intertube distance of SWNT (green triangles) and DWNT (blue circles) (derived from cryo-TEM) vs (a) PSSNa 126.7 kg/mol and (b) PSSH 75 kg/mol.

dx.doi.org/10.1021/la503287q | Langmuir 2014, 30, 14963−14970

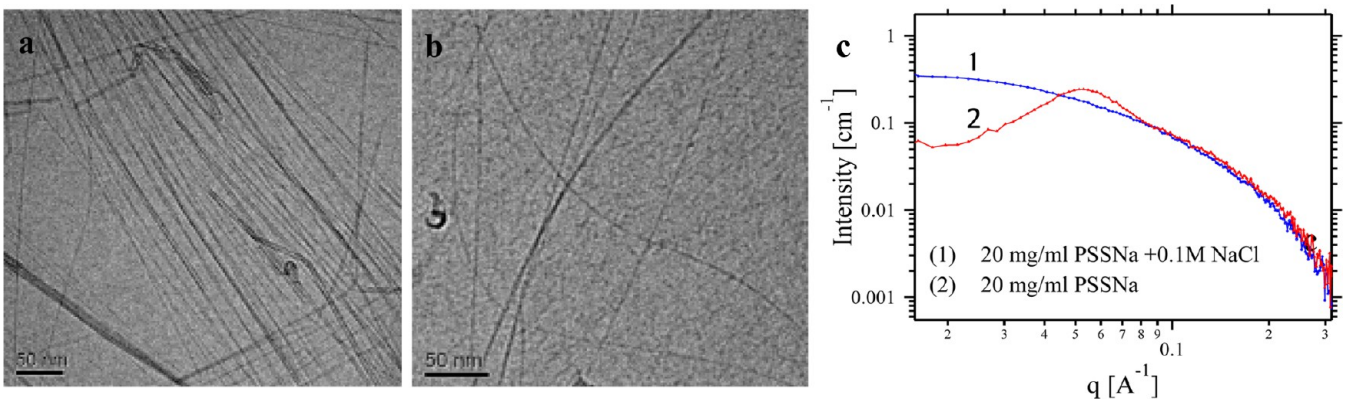

Figure 9. (a) Cryo-TEM image of 0.5 wt % SWNT dispersed in 2 wt % PSSNa 126.7 kg/mol + 0.01 M NaCl, (b) cryo-TEM image of 0.5 wt % SWNT dispersed in 2 wt % PSSNa 126.7 kg/mol + 0.1 M NaCl, and (c) SAXS intensity as a function of the scattering vector q obtained from solutions of 2 wt % PSSNa 126.7 kg/mol with 0.1 M NaCl (1) and without salt (2) (absolute intensity, after background subtraction). Scale bars are (a, b) 50 nm.

implications to confinement-induced coupling between the different components of this system are detailed in the Discussion.

At low PSS concentrations of 0.8 wt % (< 8 mg/mL), some islands of aligned SWNT can be observed. Yet, in this regime, the intertube distances are vastly varied (Figure S8, Supporting Information). At PSSNa concentrations of 0.1 wt % (1 mg/mL), the dispersed SWNT observed in cryo-TEM images are randomly oriented, and aligned SWNT are not observed. We note that in this concentration the SAXS scattering curve does not show a peak in the intensity (Figure S9, Supporting Information).

To further test the effect of electrostatic interactions on the formation of islands of aligned SWNT, NaCl was added to the dispersions at fixed polyelectrolyte concentrations. The cryo-TEM images of the dispersions showed a transition to a single phase of randomly oriented SWNT at a salt concentration of 0.1 M (Figure 9 a,b). SAXS measurements of PSS solutions showed that the scattering peak vanished at this concentration (0.1 M) (Figure 9c).

The dependence of the formation of aligned SWNT islands on the pH of the dispersions was examined as well. NaOH was added to SWNT dispersions at fixed concentration of 2 wt % PSSH (75 kg/mol). Cryo-TEM of samples prepared from the dispersions showed the presence of islands at a pH range of 2 to 13. At pH $\geq$ 13, a transition to a single phase of random networks of dispersed SWNT was observed (Figure S10, Supporting Information). The measured intertube distance did not vary with the different pH (13 $\pm$ 2 nm). SAXS measurements of polyelectrolyte solutions at different pH values showed that the scattering peak disappears at pH 13 (Figure S11, Supporting Information).

■ DISCUSSION

In this study, we report the observation via cryo-TEM of a nematic-like phase in thin films prepared from aqueous dispersions of semidilute solutions of PSS. The aligned SWNT islands appear in PSS solutions of different molecular masses and of different monovalent counterions (PSSNa, PSSH, PSSLi, and $PSSNH_3$). The micrometers-long islands of coaligned tubes coexist with a phase of randomly oriented SWNT. A similar phenomenon is observed in dispersions of DWNT but not in dispersions of MWNT of similar diameters and aspect ratios. Similar alignment of dispersed SWNT was reported by us before in solutions of spherical micelles of an ionic surfactant, CTAB;[29] other types of polymers and polyelectrolytes that were examined did not show the formation of coaligned SWNT.

The measured intertube spacing was found to depend on the polyelectrolyte concentration: as the PSS concentration increases from 2 to 8 wt %, the intertube distance was reduced from 14 to 6 nm, independent of the molecular weight of the polymer. These distances are surprisingly large when bearing in mind that a solution of a simple electrolyte of a similar concentration would have a Debye length[33] of less than 2 nm.

The coexistence of nematic and isotropic phases of dispersed SWNT at high concentration in superacids was analyzed thoroughly.[19−21] In bulk polymer solutions, one may expect that the classical models described by Onsager[16] and Flory[17,18] may be relevant. In the system described here, we observe (cryo-TEM) that self-assembled islands of coaligned tubes appear in dispersions of SWNT (below 0.5 wt %) and DWNT (d = 3 nm), whereas dispersions of MWNT (d = 6 nm) show only randomly oriented tubes at similar PSS and CNT concentrations.

We suggest that the key to rationalizing the observed behavior is related to confinement of rigid rods in a complex (structured) fluid: In the thin films prepared for cryo-TEM measurements (thickness in the range of 100−150 nm),[27] rigid rods (SWNT) that are few micrometers long are forced into a 2D configuration, whereas flexible rods (MWNT) of similar length experience a 3D environment, as they may fold in the layer. Furthermore, the confined rods (polymer-wrapped SWNT) are trapped in a semidilute solution of a polyelectrolyte with a typical intertube correlation length, ξ, dictated by the osmotic pressure of the solution.[13,14] The latter templates SWNT alignment at an intertube distance (measured by cryo-TEM) similar to the correlation length (calculated from SAXS measurements) of the bulk PSS solutions. Having the distance between the CNT being determined by the PE correlation length suggests that the parallel ordering of the tubes at this separation provokes the smallest perturbation to the PE matrix. The reason for the ordering of the long CNT is, then, the least costly perturbation to the system, as orienting the tubes results in a (not very large) loss of rotational entropy.

We note here that the solvated polyelectrolytes, with a typical persistence length of about 7 nm, do not experience confinement and follow their 3D phase diagram.[34,35]

dx.doi.org/10.1021/la503287q | Langmuir 2014, 30, 14963−14970

Consistently, we observe that confinement within a non-structured solution (SWNT in isotropic thin films, such as pluronic blockcopolymers or 0.1 M salt solutions of PSSNa) do not show the presence of nematic islands, suggesting that both confinement and the microstructure of the polymer solution are necessary conditions for inducing alignment in the SWNT.

The validity of the suggested picture depends on the difference in the rigidity of SWNT vs MWNT. Cryo-TEM images (Figure 10a) show clearly the difference in the

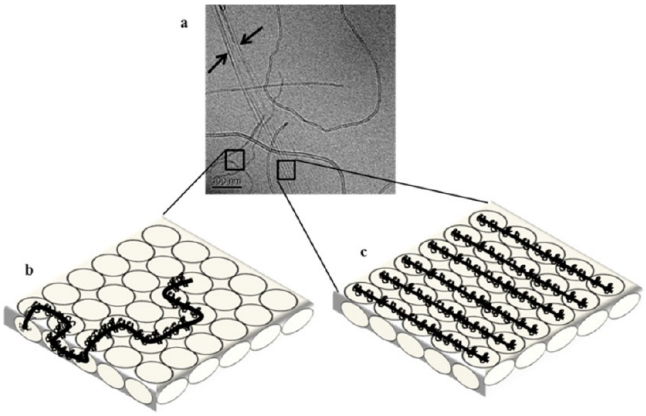

Figure 10. (a) Cryo-TEM of MWNTs and SWNT dispersed in 2 wt % PSSH 75 kg/mol. The arrows point to a nematic-like SWNT island. (b) Schematic drawing of the MWNT dispersed in PSSH solution. (c) Schematic drawing of the SWNT nematic island in PSSH solution. The ellipses represent the mesh size of the polymer solution. Scale bar (a) is 100 nm.

persistence length of SWNT and MWNT (see schematic drawing in Figure 10b,c). The experimentally measured persistence length for SWNT ranges from 32 to 174 μm[5] and longer, suggesting that the tubes investigated in this study behave as rigid rods. In the case of MWNT a thorough analysis of CVD-grown MWNT suggests that their rheological behavior is well-described by a worm-like coil model with a bending persistence length in the range of 200 nm.[6]

We find that, in the nematic islands, the intertube distance does not depend on the molecular weight and counterion type of the PE. This observation is consistent with the fact that the correlation length of polyelectrolytes in the semidilute regime does not depend on the two parameters.[36]

What is the nature of the observed phenomenon? Are the observed coexisting phases at equilibrium, implying an equality of the osmotic pressure and the chemical potential in the two phases, or are they transient phases induced by sample preparation? The on-the-grid shear–relaxation experiments presented in this study (Figure 5) support the assumption that the observed phases are long-lived metastable phases or equilibrium states. If so, then can the analogy be made with the isotropic–nematic transition discussed by the classical models mentioned above?[16,17] Probably not, as we find that at the very same concentration of SWNT but low polyelectrolyte concentration where the PE solution is homogeneous (PSSNa 0.1 wt %; Figure S9, Supporting Information) similar islands are not observed. The dimensionality of the confined systems introduces an additional complication to the interpretation of the experimental observations, as the nature of isotropic–nematic transition in two-dimensional systems is more complicated and not yet well understood.[37]

We suggest that the presence of the nematic-like islands can be rationalized by two possible explanations. The first one is self-assembly of the SWNT, which is templated by the presence of the solvated polyelectrolytes. The clear role of the microstructure polyelectrolyte phase is highlighted by the experiments at low PE concentration or high salt concentrations (Figure 9) that show that in isotropic solutions of PE, and the very same SWNT concentrations, islands of nematic-like order are not observed. Furthermore, the experimental evidence clearly shows that the intertube distance is determined by the polyelectrolyte solution's properties, i.e., the correlation length of the PE. Although this is our preferred explanation, we cannot rule out that what we are observing is the appearance of finite size clusters that arise from a two-dimensional isotropic–nematic transition. The clusters suggest that the transition is first-order, and they represent either sizes below the critical nucleation size or clusters whose growth has been arrested by kinetic barriers. Complete characterization of the nature of the transition and a distinction between self-assembly and a first-order phase transition require a thorough experimental work, which is well-beyond the scope of the present article.

■ CONCLUSIONS

The phase behavior of CNT in polyelectrolyte solution is very complex and depends not only on the CNT concentration but also on the intertube potential, the adsorbed and freely solvated PE, the counterions, and the solvent. We find that under an external constraint, such as confinement into a thin film, microstructured PE solutions may template the formation of micrometers-long islands of orientationally ordered SWNT at low SWNT concentrations. This observation offers a new pathway for the design of nonisotropic coating layers for optical and electrical applications.

■ ASSOCIATED CONTENT

Supporting Information

Characteristics of the different types of CNT and polymers used in the experiments; cryo-TEM images of SWNT dispersed in different molecular masses of PSSNa, following on-the-grid relaxation, SWNT dispersed in PSS in the dilute regime, and SWNT dispersion in 2 wt % PSSH at pH 2–13; SAXS results of 2 wt % PSSH at pH 2 and 13 and of dispersions of DWNT and MWNT in PSSNa; rheology of PSSNa solution and dispersions of SWNT in PSSNa; logarithmic plot of the correlation length vs PSSH concentration. This material is available free of charge via the Internet at http://pubs.acs.org.

■ AUTHOR INFORMATION

Corresponding Author

*E-mail: rachely@bgu.ac.il.

Notes

The authors declare no competing financial interest.

■ ACKNOWLEDGMENTS

R.Y.-R. holds the Stanley D. and Nikki Waxberg professorial chair in Advanced Materials. The support of the Israel Science Foundation is acknowledged. I.S. acknowledges support from the National Science Foundation under grant CBET-1403058.

REFERENCES

(1) Bandyopadhyaya, R.; Nativ-Roth, E.; Regev, O.; Yerushalmi-Rozen, R. Stabilization of Individual Carbon Nanotubes in Aqueous Solutions. *Nano Lett.* **2002**, *2*, 25−28.

(2) *Carbon Nanotubes: Advanced Topics in the Synthesis, Structure, Properties and Applications*; Jorio, A., Dresselhaus, G., Dresselhaus, M. S., Eds.; Springer-Verlag: New York, 2007; Vol. *111*.

(3) Joachim, C.; Gimzewski, J.; Aviram, A. Electronics Using Hybrid-Molecular and Mono-Molecular Devices. *Nature* **2000**, *408*, 541−548.

(4) Moniruzzaman, M.; Winey, K. I. Polymer Nanocomposites Containing Carbon Nanotubes. *Macromolecules* **2006**, *39*, 5194−5205.

(5) Green, M. J.; Behabtu, N.; Pasquali, M.; Adams, W. W. Nanotubes as Polymers. *Polymer* **2009**, *50*, 4979−4997.

(6) Lee, H. S.; Yun, C. H.; Kim, H. M.; Lee, C. J. Persistence Length of Multiwalled Carbon Nanotubes with Static Bending. *J. Phys. Chem. C* **2007**, *111*, 18882−18887.

(7) Nativ-Roth, E.; Shvartzman-Cohen, R.; Bounioux, C.; Florent, M.; Zhang, D.; Szleifer, I.; Yerushalmi-Rozen, R. Physical Adsorption of Block Copolymers to SWNT and MWNT: A Nonwrapping Mechanism. *Macromolecules* **2007**, *40*, 3676−3685.

(8) Rubianes, M. D.; Rivas, G. A. Dispersion of Multi-Wall Carbon Nanotubes in Polyethylenimine: A New Alternative for Preparing Electrochemical Sensors. *Electrochem. Commun.* **2007**, *9*, 480−484.

(9) Manesh, K.; Kim, H. T.; Santhosh, P.; Gopalan, A.; Lee, K. A Novel Glucose Biosensor Based on Immobilization of Glucose Oxidase into Multiwall Carbon Nanotubes−Polyelectrolyte-Loaded Electrospun Nanofibrous Membrane. *Biosens. Bioelectron.* **2008**, *23*, 771−779.

(10) Sinani, V. A.; Gheith, M. K.; Yaroslavov, A. A.; Rakhnyanskaya, A. A.; Sun, K.; Mamedov, A. A.; Wicksted, J. P.; Kotov, N. A. Aqueous Dispersions of Single-Wall and Multiwall Carbon Nanotubes with Designed Amphiphilic Polycations. *J. Am. Chem. Soc.* **2005**, *127*, 3463−3472.

(11) O'Connell, M. J.; Boul, P.; Ericson, L. M.; Huffman, C.; Wang, Y.; Haroz, E.; Kuper, C.; Tour, J.; Ausman, K. D.; Smalley, R. E. Reversible Water-Solubilization of Single-Walled Carbon Nanotubes by Polymer Wrapping. *Chem. Phys. Lett.* **2001**, *342*, 265−271.

(12) Dobrynin, A. V.; Rubinstein, M. Theory of Polyelectrolytes in Solutions and at Surfaces. *Prog. Polym. Sci.* **2005**, *30*, 1049−1118.

(13) De Gennes, P. d.; Pincus, P.; Velasco, R.; Brochard, F. Remarks on Polyelectrolyte Conformation. *J. Phys.* **1976**, *37*, 1461−1473.

(14) Colby, R. H. Structure and Linear Viscoelasticity of Flexible Polymer Solutions: Comparison of Polyelectrolyte and Neutral Polymer Solutions. *Rheol. Acta* **2010**, *49*, 425−442.

(15) Dror, Y.; Pyckhout-Hintzen, W.; Cohen, Y. Conformation of Polymers Dispersing Single-Walled Carbon Nanotubes in Water: A Small-Angle Neutron Scattering Study. *Macromolecules* **2005**, *38*, 7828−7836.

(16) Onsager, L. The Effects of Shape on the Interaction of Colloidal Particles. *Ann. N.Y. Acad. Sci.* **1949**, *51*, 627−659.

(17) Flory, P. J. Phase Equilibria in Solutions of Rod-Like Particles. *Proc. R. Soc. London, Ser. A* **1956**, *234*, 73−89.

(18) Flory, P. J.; Abe, A. Statistical Thermodynamics of Mixtures of Rodlike Particles. 1. Theory for Polydisperse Systems. *Macromolecules* **1978**, *11*, 1119−1122.

(19) Rai, P. K.; Pinnick, R. A.; Parra-Vasquez, A. N. G.; Davis, V. A.; Schmidt, H. K.; Hauge, R. H.; Smalley, R. E.; Pasquali, M. Isotropic-Nematic Phase Transition of Single-Walled Carbon Nanotubes in Strong Acids. *J. Am. Chem. Soc.* **2006**, *128*, 591−595.

(20) Davis, V. A.; Ericson, L. M.; Parra-Vasquez, A. N. G.; Fan, H.; Wang, Y.; Prieto, V.; Longoria, J. A.; Ramesh, S.; Saini, R. K.; Kittrell, C. Phase Behavior and Rheology of SWNTs in Superacids. *Macromolecules* **2004**, *37*, 154−160.

(21) Davis, V. A.; Parra-Vasquez, A. N. G.; Green, M. J.; Rai, P. K.; Behabtu, N.; Prieto, V.; Booker, R. D.; Schmidt, J.; Kesselman, E.; Zhou, W. True Solutions of Single-Walled Carbon Nanotubes for Assembly into Macroscopic Materials. *Nat. Nanotechnol.* **2009**, *4*, 830−834.

(22) Song, W.; Windle, A. H. Isotropic-Nematic Phase Transition of Dispersions of Multiwall Carbon Nanotubes. *Macromolecules* **2005**, *38*, 6181−6188.

(23) Zhang, S.; Kinloch, I. A.; Windle, A. H. Mesogenicity Drives Fractionation in Lyotropic Aqueous Suspensions of Multiwall Carbon Nanotubes. *Nano Lett.* **2006**, *6*, 568−572.

(24) Islam, M.; Alsayed, A.; Dogic, Z.; Zhang, J.; Lubensky, T.; Yodh, A. Nematic Nanotube Gels. *Phys. Rev. Lett.* **2004**, *92*, 088303.

(25) Shvartzman-Cohen, R.; Nativ-Roth, E.; Baskaran, E.; Levi-Kalisman, Y.; Szleifer, I.; Yerushalmi-Rozen, R. Selective Dispersion of Single-Walled Carbon Nanotubes in the Presence of Polymers: The Role of Molecular and Colloidal Length Scales. *J. Am. Chem. Soc.* **2004**, *126*, 14850−14857.

(26) Danino, D.; Talmon, Y.; Zana, R. Cryo-TEM of Thread-Like Micelles: On-the-Grid Microstructural Transformations Induced during Specimen Preparation. *Colloids Surf., A* **2000**, *169*, 67−73.

(27) Cho, H.-J.; Hyun, J.-K.; Kim, J.-G.; Seop Jeong, H.; Park, H.N.; You, D.-J.; Jung, H.S. Measurement of Ice Thickness on Vitreous Ice Embedded Cryo-EM Grids: Investigation of Optimizing Condition for Visualizing Macromolecules. *J. Anal. Sci. Technol.* **2013**, *4*, 7.

(28) Nativ-Roth, E.; Regev, O.; Yerushalmi-Rozen, R. Shear-Induced Ordering of Micellar Arrays in the Presence of Single-Walled Carbon Nanotubes. *Chem. Commun.* **2008**, 2037−2039.

(29) Nativ-Roth, E.; Nap, R. J.; Szleifer, I.; Yerushalmi-Rozen, R. Order−Disorder Transition Induced by Surfactant Micelles in Single-Walled Carbon Nanotubes Dispersions. *Soft Matter* **2010**, *6*, 5289−5292.

(30) Zheng, Yi.; Lin, Z.; Zakin, J.L; Talmon, Y.; Davis, H.T.; Scriven, L.E Cryo-TEM Imaging the Flow-Induced Transition from Vesicles to Threadlike Micelles. *J. Phys. Chem. B* **2000**, *104*, 5263−5271.

(31) Ben-David, O.; Nativ-Roth, E.; Yerushalmi-Rozen, R.; Gottlieb, M. Rheological Investigation of Single-Walled Carbon Nanotubes-Induced Structural Ordering in CTAB Solutions. *Soft Matter* **2009**, *5*, 1925−1930.

(32) Nierlich, M.; Williams, C.; Boue, F.; Cotton, J.; Daoud, M.; Famoux, B.; Jannink, G.; Picot, C.; Moan, M.; Wolff, C. Small Angle Neutron Scattering by Semi-Dilute Solutions of Polyelectrolyte. *J. Phys.* **1979**, *40*, 701−704.

(33) Evans, D. F.; Wennerström, H. *The Colloidal Domain: Where Physics Chemistry, Biology, and Technology Meet*; John Wiley & Sons: New York, 1999; Vol. *2*, pp 193−197.

(34) *Liquid Crystallinity in Polymers: Principles and Fundamental Properties*; Ciferri, A., Ed.; VCH Publishers: New York, 1991.

(35) Belloni, L.; Drifford, M.; Turq, P. Counterion Diffusion in Polyelectrolyte Solutions. *Chem. Phys.* **1984**, *83*, 147−154.

(36) Kaji, K.; Urakawa, H.; Kanaya, T.; Kitamaru, R. Phase Diagram of Polyelectrolyte Solutions. *J. Phys.* **1988**, *49*, 993−1000.

(37) Barci, D.G.; Stariolo, D.A. Competing Interactions, the Renormalization Group, and the Isotropic-Nematic Phase Transition. *Phys. Rev. Lett.* **2007**, *L 98*, 200604.